

# Screening Effects in Solutions of a Hyperbranched, Dendrimer-Like Polyester

Rittirong Pruthikul, Michael M. Coleman, and Paul C. Painter\*

Department of Material Science and Engineering, The Pennsylvania State University, University Park, Pennsylvania 16802

Nora Beck Tan

U.S. Army Research Laboratory, Aberdeen Proving Ground, Maryland 21005

Received June 26, 2000; Revised Manuscript Received February 1, 2001

**ABSTRACT:** We have previously shown that infrared spectroscopy can be used to “count” the number of contacts in hydrogen-bonded system. We use such information to determine appropriate self- and interassociation equilibrium constant values and at the same time take into account the intramolecular “screening” in polymer blends and solutions. The calculated values reported here for screening, and hence the accessibility of the functional groups in a hyperbranched polyester, are based on the interassociation equilibrium constants obtained from the low molecular weight counterparts of the hyperbranched repeat units and give a measure of the accessibility of functional groups in these highly branched systems.

## Introduction

Recent work in this laboratory has focused on what we call “screening and spacing effects” in solutions and blends of linear polymers.<sup>1–7</sup> Essentially, a chain bends back on itself, largely through local as opposed to long-range effects, so that there are a greater number of like-like contacts in polymer blends and solutions than would be predicted on the basis of a random mixing of segments.<sup>2</sup> These effects alter the ability of functional groups to hydrogen bond to partners. With the unique ability of infrared spectroscopy to “count” the number of contacts in well-chosen hydrogen-bonded systems, we have been able to quantify this effect in various mixtures.<sup>1</sup> We are now concerned with an extension of this work, the effect of microstructure or molecular architecture on the number of contacts, and hence the intermolecular interaction term. An intriguing example of this involves blends and solutions of hyperbranched polymers and dendrimers.

Dendrimers are highly branched structures consisting of a central core from which treelike arms extend three-dimensionally into space. The number of branches increases systematically from the core of the molecule in a radial (topological) direction. Each successive layer of branches is called a generation. Initial theoretical work by de Gennes and Hervet<sup>8</sup> suggested a dense-shell model, where the end groups are located near the periphery of the molecule with a density that increases sharply with generation number. More recent simulations using various approaches<sup>9–13</sup> suggests that the lower generation dendrimers ( $g \leq 4$ ) indeed have an open structure, with the chain ends located near the periphery. However, by the fifth generation there is a more spherical three-dimensional structure with an approximately uniform density of end groups distributed throughout the molecule. This inward folding of the chain-ends was also supported by recent experimental NMR work by Wooley et al.<sup>14</sup> on a fifth generation dendrimer.

In preliminary work, we characterized solutions and blends of a hyperbranched dendrimer-like polyester<sup>15</sup> whose structure is illustrated in Figure 1. To probe the

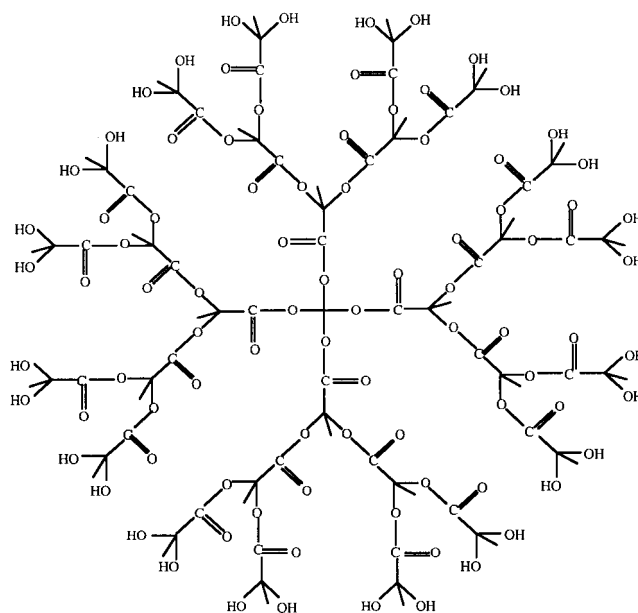


**Figure 1.** Schematic representation of a dendrimer.

number of contacts and also distinguish between the accessibility of terminal end groups and those within the core, we converted the peripheral OH groups to esters by reacting with <sup>13</sup>C-labeled acetyl chloride. The resulting <sup>13</sup>C=O stretching mode was well separated from its <sup>12</sup>C counterpart (near 1700 and 1740 cm<sup>-1</sup>, respectively), allowing us to demonstrate that the terminal end groups are much more accessible than their internal counterparts. This may not at first appear too surprising, but recall that modeling of pure dendrimers indicates that by the fifth generation there is a more-or-less uniform distribution of end groups throughout the molecule, which in turn suggests that even in the concentrated regime, where our studies were conducted, the conformation of the molecules become more extended in solution, so that the end groups are located more toward the periphery than folded into the core of the molecule.

An obvious extension of our initial experiments is to study the degree of hydrogen bonding and hence number of contacts as a function of generation number, as simulations indicate that the lower generation molecules ( $g \leq 4$ ) have a more open, extended structure. That is what we will report here.

## Experimental Section

Generations 2, 4, and 5 of an aliphatic hyperbranched polyester with hydroxyl terminal groups were provided by Perstorp Polyols Inc. and used as received. Dendritic growth in these materials is controlled by the stoichiometry of the reactants and the polymers are presumably polydisperse. Nevertheless, the ratio of end groups to internal functional groups detected by infrared spectroscopy is close to what would be expected for a perfect dendritic structure.<sup>15</sup>

4-Ethylphenol (EPh), cyclohexane (CHEX), and tetrahydrofuran (THF) were obtained from Aldrich and used as received. Methyl trimethyl acetate (MTA) with a boiling point of 101 °C and methyl acetate (MAc) with a boiling point of 57.5 °C were purchased from Aldrich and distilled before use. <sup>13</sup>C acetyl chloride was purchased from Cambridge Isotope Laboratories, Inc. Acetylation of the terminal OH groups to form esters was accomplished by refluxing in THF overnight at 60 °C. The products were precipitated in water, collected and dried under vacuum at room temperature.

Hyperbranched polymer/EPh solutions were prepared by weight. The tacky solutions were then smeared on and pressed between two KBr windows to obtain films of uniform thickness and hence flat baselines in the infrared spectra. Dilute MTA/EPh and MAc/EPh solutions in CHEX were prepared in volumetric flasks. They were then introduced into sealed KBr liquid cells with a path length of 0.5 mm. All infrared spectra were recorded on a Digilab model FTS-45 Fourier transform infrared (FTIR) spectrometer at a resolution of 2 cm<sup>-1</sup>. Great care has been taken to ensure that infrared absorption is within the Beer-Lambert law range, otherwise band distortions are likely to occur.<sup>16</sup>

## Results and Discussion

**Spectroscopy of the Hyperbranched Polyester/Ethyl Phenol Mixtures.** We will consider mixtures of our hyperbranched polyester with ethylphenol, EPh. In such mixtures there will be an equilibrium distribution of hydrogen-bonded and free carbonyl groups that will vary systematically with composition and temperature and will depend on functional groups accessibility. As we have shown in numerous previous studies of mixture involving phenolic OH and ester carbonyl groups, this distribution can be described in terms of equilibrium constants. Two of these describe the self-association of EPh and are determined by spectroscopic studies of this molecule in an "inert" (non hydrogen bonding) solvent (e.g., cyclohexane), and the other (interassociation) equilibrium constant describes the phenolic OH/ester carbonyl hydrogen bond that is obtained from a measure of the fraction of the free and bonded groups that are obtained by direct infrared studies of the mixtures. We have previously obtained self-association constants for EPh and all we have to consider here is the interassociation constant.

The carbonyl stretching region of the infrared spectra of mixtures of EPh with generation 2 (g 2) and generation 5 (g 5) hyperbranched polyester are shown in Figures 2 and 3, respectively. The compositions of the solutions varied from 65% EPh by weight (65/35) to 35% (35/65). Although it would have been advantageous in terms of spectroscopic measurements to also include solutions of higher EPh content in our studies, we were concerned that we would essentially "saturate" the

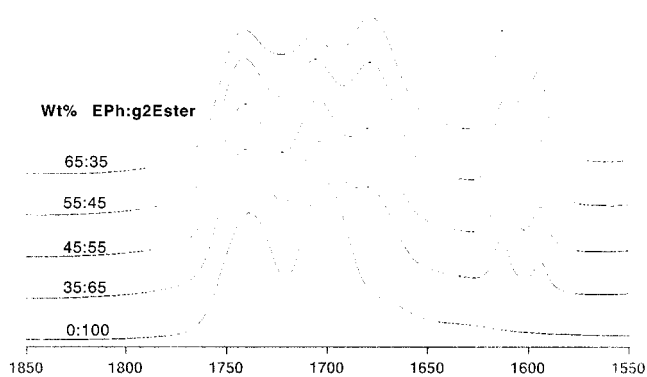


**Figure 2.** FTIR spectra of the carbonyl-stretching region of hyperbranched ester generation 2 in concentrated EPh solutions.

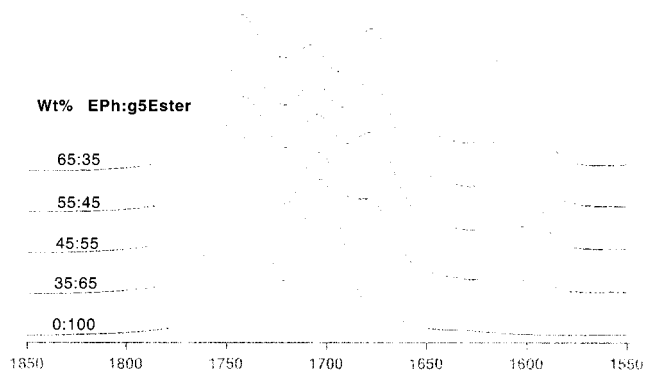


**Figure 3.** FTIR spectra of the carbonyl-stretching region of hyperbranched ester generation 5 in concentrated EPh solutions.

hyperbranched molecules. Because of their architecture, the overlap threshold for these polymers occurs at a much higher concentration than for linear chains and making measurements on mixture where these dendrimer-like entities are essentially separated in a sea of EPh would affect our calculation of equilibrium constants.

The spectra shown in Figures 2 and 3 compare the solution spectra to that of the pure <sup>13</sup>C acetylated sample. As mentioned above, the latter has two bands, near 1740 and 1700 cm<sup>-1</sup>, characteristic of the free <sup>12</sup>C and <sup>13</sup>C carbonyl stretching modes, respectively. As we showed in previous work,<sup>15</sup> two additional modes appear in the solution spectra, near 1724 and 1678 cm<sup>-1</sup>, characteristic of hydrogen-bonded groups. Unfortunately, the 1724 cm<sup>-1</sup> hydrogen-bonded carbonyl band of the <sup>12</sup>C groups overlaps the "free" band of <sup>13</sup>C group, so that in this region of the spectrum there appears to be just three bands. Partly as a result of this there does not appear to be a large difference in the spectra of the g 2 and g 5 samples at first sight, but if the spectra of the 65% EPh solutions (labeled 65:35 in the figure) are examined carefully, there is clearly a larger fraction of <sup>13</sup>C hydrogen-bonded groups (1678 cm<sup>-1</sup> band) in the g 2 sample than the g 5.

A quantitative comparison and the determination of equilibrium constants requires careful curve-resolving of the spectral profiles. We discussed this in detail in our preliminary study of these polymers. Essentially, we have prior knowledge of the characteristics of certain bands (frequency, width at half-height, band shape) from the spectra of the pure materials and <sup>12</sup>C acetylated samples, where there are just two bands (free and bonded). Furthermore, the <sup>13</sup>C hydrogen-bonded band

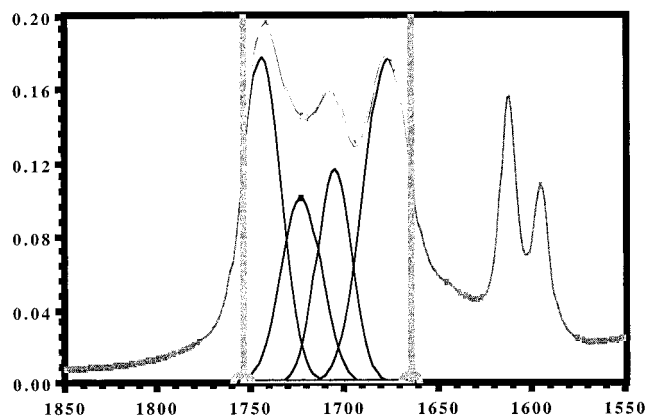


**Figure 4.** Example of curve resolving from the carbonyl stretching region of 35% hyperbranched ester generation 5 in EPh solution.

**Table 1.** Curve-Resolving Data for Concentrated EPh Solutions of Hyperbranched Ester

polymer	composition wt % of EPh	vol fract of EPh, $\Phi_B$	mole fraction of HB carbonyl	
			$^{12}\text{C}$	$^{13}\text{C}$
generation 2	35	0.43	0.13	0.43
	45	0.53	0.20	0.52
	55	0.63	0.27	0.60
	65	0.72	0.32	0.65
generation 4	35	0.43	0.14	0.42
	45	0.53	0.22	0.49
	55	0.63	0.27	0.55
	65	0.72	0.32	0.61
generation 5	35	0.43	0.15	0.39
	45	0.53	0.23	0.47
	55	0.63	0.27	0.52
	65	0.72	0.30	0.59

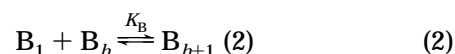
near 1678  $\text{cm}^{-1}$  is well-defined, and these factors, coupled with consistency in procedure, experience, and common sense allow us to curve resolve the bands with what we believe is a reasonable degree of accuracy. An example of this curve resolving is shown in Figure 4, and the fraction of hydrogen-bonded groups is presented in Table 1.

These results show that the fraction of hydrogen-bonded groups increases systematically with EPh concentration, as it should providing we do not "saturate" the hyperbranched polymers, at which point we would expect the measured fraction of hydrogen-bonded groups to level off. As might be anticipated, the fraction of hydrogen bonds formed on the terminal carbonyl groups ( $^{13}\text{C}$ ) are much larger than their ( $^{12}\text{C}$ ) internal counterparts, suggesting that the structure are at least somewhat extended in solutions rather than being compact in shape. However, the degree of hydrogen bonding on the  $^{13}\text{C}$  terminal carbonyl groups does appear to decrease slightly as the generation number increases, indicating that at least to some small degree the chains fold back on themselves in the higher generation samples. This result is not inconsistent with the simulations performed on athermal systems, in that hydrogen bonding may provide a strong driving force for unfolding of these molecules even in the concentrated regime.

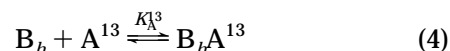
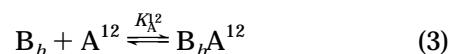
The numerical results on hydrogen bonding of the internal ( $^{12}\text{C}$ ) carbonyl bands in all three generations are very similar, indicating equivalent penetration of EPh molecules into the interior of these macromolecules.

**Calculating Equilibrium Constants.** To further analyze these data and to compare the data directly

with the fraction of hydrogen bonds formed in blends and solutions of linear polymers, we evaluated the inter-association equilibrium constants,  $K_A^{12}$  and  $K_A^{13}$ , by fitting the experimental data to stoichiometric equations. The calculations start from the self-association of EPh which can be adequately described by two equilibrium constants:  $K_2$  represents the formation of dimers and  $K_B$ , the formation of multimers, as depicted below:



The acetylated hyperbranched ester groups, defined as  $A^{12}$  and  $A^{13}$  in accordance with their  $^{12}\text{C}$  and  $^{13}\text{C}$  labels, do not self-associate through hydrogen bonds, but are "acceptors" for the  $-\text{OH}$  proton of EPh. These hydrogen bonds are described by the equilibrium constants  $K_A^{12}$  and  $K_A^{13}$ , respectively:



The competing (dimensionless) equilibrium constants,  $K_A^{12}$  and  $K_A^{13}$ , are defined as in our previous work as follows:

$$K_A^{12} = \left( \frac{\Phi_{B_h A^{12}}}{\Phi_{B_h} \Phi_{A^{12}}} \right) \left( \frac{r_A^{12} h}{h + r_A^{12}} \right) \quad (5)$$

$$K_A^{13} = \left( \frac{\Phi_{B_h A^{13}}}{\Phi_{B_h} \Phi_{A^{13}}} \right) \left( \frac{r_A^{13} h}{h + r_A^{13}} \right) \quad (6)$$

Here we let the volume fraction of the self-associating component be  $\Phi_B$ , while that of the ester is  $\Phi_A$ . All subscripts denote hydrogen-bonded species, while additional superscripts 12 and 13 account for  $^{12}\text{C}$  and  $^{13}\text{C}$  labeling.  $\Phi_{A_1}$  and  $\Phi_{B_1}$  represent the volume fraction of A and B segments that are not hydrogen bonded at any instant. The quantities  $r_A^{12}$  and  $r_A^{13}$  are the ratios of the respective molar volumes of the A and B segments:

$$r_A^{12} = \frac{V_A^{12}}{V_B} \quad (7)$$

$$r_A^{13} = \frac{V_A^{13}}{V_B} \quad (8)$$

The stoichiometric equations, relating the concentration of ester segments and EPh molecules to hydrogen-bonded species are as given in our previous work:

$$\Phi_A^{12} = \Phi_{A_1} [1 + K_A^{12} \Phi_{B_1}] \quad (9)$$

$$\Phi_A^{13} = \Phi_{A_1} [1 + K_A^{13} \Phi_{B_1}] \quad (10)$$

$$\Phi_B = \Phi_{B_1} \Gamma_2 \left[ 1 + \frac{K_A^{12} \Phi_{A_1}^{12}}{r_A^{12}} + \frac{K_A^{13} \Phi_{A_1}^{13}}{r_A^{13}} \right] \quad (11)$$

Here

$$\Gamma_1 = \left(1 - \frac{K_2}{K_B}\right) + \frac{K_2}{K_B} \left(\frac{1}{(1 - K_B \Phi_{B_1})}\right) \quad (12)$$

$$\Gamma_2 = \left(1 - \frac{K_2}{K_B}\right) + \frac{K_2}{K_B} \left(\frac{1}{(1 - K_B \Phi_{B_1})^2}\right) \quad (13)$$

The quantities  $\Phi_A^{12}$ ,  $\Phi_A^{13}$ ,  $\Phi_B$ ,  $\Gamma_A^{12}$ ,  $\Gamma_A^{13}$  are all known while  $K_2$  and  $K_B$  are obtained from studies of EPh in an "inert" solvent. Moreover,  $\Phi_{A_1}^{12}$  and  $\Phi_{A_1}^{13}$  are the quantities evaluated from curve-resolving (the fraction free =  $\Phi_{A_1}/\Phi_A$ ). We are left with three unknowns  $\Phi_{B_1}$ ,  $K_A^{12}$ , and  $K_A^{13}$ . With three stoichiometric equations in hand, i.e., eqs 9–11, it is possible to solve for  $\Phi_{B_1}$ ,  $K_A^{12}$ , and  $K_A^{13}$  at each composition.

Although the calculated values of  $K_A^{12}$  and  $K_A^{13}$  can be used to determine phase behavior, they differ from those obtained from low molecular weight analogues, polymer solutions, or blends, because of what we have called screening and other effects. The frequency shifts observed in the infrared spectra indicates that the strength (enthalpy) of the phenolic OH/ester carbonyl hydrogen bonds is the same in all of the systems we have examined (apart from those where bulky groups provide steric hindrance). The accessibility of the functional groups, and hence the number of hydrogen bonds that can be formed, is very different, however, and depends on chain architecture. To account for this we have defined "intrinsic" equilibrium constants, that are characteristic of hydrogen bonds in the functional groups in question, then introduced factors that account for the accessibility of the functional groups, hence screening etc. We have described this in previous work but need to modify the equations slightly here. The algebra is not that complex, but there are a lot of terms. What we will end up with is simple, however. The stoichiometric equations will remain exactly the same as those given above, except the equilibrium constants,  $K_B$ ,  $K_A$  etc., will be replaced by "apparent" equilibrium constants,  $\tilde{K}_A$ ,  $\tilde{K}_B$ . These will be related to the intrinsic equilibrium constants, now designated  $K_B$ ,  $K_A$  through a factor  $\gamma$ , that accounts for both chain connectivity and intramolecular screening.

We start by defining the number of neighbors to a chain, following Guggenheim

$$qz = M(z - 2) + 2 \quad (14)$$

where  $M$  is the number of repeat units on a chain and  $z$  is the number of neighbors to a lattice cell. Note that for branched molecules this definition does not change, in that every branch point is accompanied by an additional end group. This can be rewritten as

$$\frac{q}{M} = 1 - \frac{2}{z} \left(1 + \frac{1}{M}\right) \quad (15)$$

$$\frac{q}{M} \equiv 1 - \gamma_1 \quad (16)$$

We define  $\Theta$  as the surface site fraction. For our hyperbranched polyester in EPh solution, we can write

$$\Theta_B = \frac{\Phi_B}{\Phi_B + (1 - \gamma_1^{A12})\Phi_A^{12} + (1 - \gamma_1^{A13})\Phi_A^{13}} \quad (17)$$

Note that the  $\Phi_B$  term does not have a  $1 - \gamma_1$  factor because EPh molecules are not polymeric.

If we define

$$\langle \gamma_1 \Phi_A \rangle \equiv \gamma_1^{A12} \Phi_A^{12} + \gamma_1^{A13} \Phi_A^{13} \quad (18)$$

it follows that

$$\Theta_B = \frac{\Phi_B}{1 - \langle \gamma_1 \Phi_A \rangle} \quad (19)$$

$$\Theta_A^{12} = \frac{\Phi_A^{12}(1 - \gamma_1^{A12})}{1 - \langle \gamma_1 \Phi_A \rangle} \quad (20)$$

$$\Theta_A^{13} = \frac{\Phi_A^{13}(1 - \gamma_1^{A13})}{1 - \langle \gamma_1 \Phi_A \rangle} \quad (21)$$

Next, we define  $P_{BB}$  as the probability of a B–B contact, which is determined by the number of neighbors to B segments. At this point, we also add another factor, which accounts for intramolecular screening of the A (polyester) molecules. The fraction of same chain contacts is  $\gamma_s^A$ , so we now find a factor  $(1 - \gamma_s^A)$  to account for the reduction of AB intermolecular contacts (as before, there is no equivalent factor for the B molecules because they are not polymeric):

$$P_{BB} = \frac{\Theta_B}{\Theta_B + (1 - \gamma_s^{A12})\Theta_A^{12} + (1 - \gamma_s^{A13})\Theta_A^{13}} \quad (22)$$

Through some rearranging, we have

$$P_{BB} = \frac{\Phi_B}{1 - \gamma^{12}\Phi_A^{12} - \gamma^{13}\Phi_A^{13}} \quad (23)$$

$$P_{A^{12}B} = \frac{\Phi_A^{12}(1 - \gamma^{12})}{1 - \gamma^{12}\Phi_A^{12} - \gamma^{13}\Phi_A^{13}} \quad (24)$$

$$P_{A^{13}B} = \frac{\Phi_A^{13}(1 - \gamma^{13})}{1 - \gamma^{12}\Phi_A^{12} - \gamma^{13}\Phi_A^{13}} \quad (25)$$

where we have defined

$$\gamma^{12} \equiv \gamma_1^{A12} + \gamma_s^{A12}(1 - \gamma_1^{A12}) \quad (26)$$

$$\gamma^{13} \equiv \gamma_1^{A13} + \gamma_s^{A13}(1 - \gamma_1^{A13}) \quad (27)$$

We now can rewrite the expressions for our "apparent" equilibrium constants in terms of the intrinsic equilibrium constants as

$$\tilde{K}_A^{12} = K_A^{12} \frac{P_{A^{12}B}}{\Phi_A^{12}} \quad (28)$$

$$\tilde{K}_A^{13} = K_A^{13} \frac{P_{A^{13}B}}{\Phi_A^{13}} \quad (29)$$



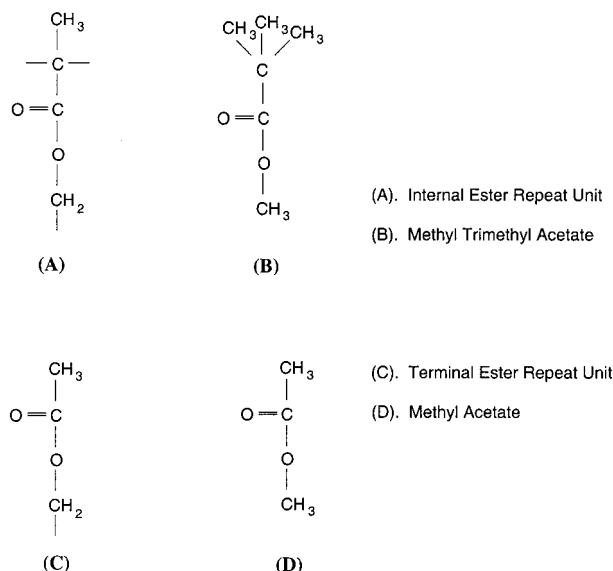


**Figure 5.** Schematic representations of the hyperbranched repeat units and their low molecular weight counterparts.

Obviously, problems arise as soon as we introduce additional parameters into our calculations. We originally had three equations and three unknowns for each composition. We now have the same three stoichiometric equations and five unknowns, namely  $\Phi_{B1}$ ,  $K_A^{12}$ ,  $K_A^{13}$ ,  $\gamma^{12}$ , and  $\gamma^{13}$ . As a result, we would have to obtain solutions by an iterative calculation using data from all four compositions.

Because of possible errors in curve-resolving and the iterative procedure used in our calculations, we were concerned that a number of almost equally valid solutions could be obtained. We therefore conducted experiments on dilute (in cyclohexane, CHEX) solutions of Eph with low molecular weight counterparts of the hyperbranched ester, methyl trimethyl acetate, TMA, and methyl acetate, MAc, whose structures are very similar to segments of the internal and terminal repeat units of the hyperbranched polyester respectively, as illustrated in Figure 5. Such experiments would give us the intrinsic values of  $K_A^{12}$  and  $K_A^{13}$ , once again leaving us in the position of having three stoichiometric equations and three unknowns for each composition.

**Low Molecular Weight Analogues.** The experimental procedure used to measure  $K_A$  values for Eph/MTA and Eph/MAc solutions is similar to that previously used in our laboratory.<sup>7</sup> Because we are using sealed cell of known thickness, we can directly calculate the absolute absorptivity of the free carbonyl band,  $a_F^{C=O}$  as

$$a_F^{C=O} = \frac{A_F^{C=O}}{bc} \quad (30)$$

Hence

$$\epsilon_F^{C=O} = \frac{A_F^{C=O}}{a_F^{C=O} bc} \quad (31)$$

This allows us to disregard the details of the complicated hydrogen-bonded bands that often appear in dilute solutions (because of cooperative effects). Curve-resolving is still used to separate any overlap of the free and the bonded bands, but this can be done very accurately,

**Table 2.** Curve-Resolving Data for Diluted Eph Solutions of Methyl Trimethyl Acetate in CHEX

vol fract Eph	vol fract MTA	fract of free carbonyl
0.002 39	0.001 28	0.821
0.002 59	0.001 60	0.810
0.002 64	0.001 60	0.805
0.005 18	0.001 59	0.720
0.005 27	0.001 60	0.734
0.006 59	0.001 60	0.686
0.007 91	0.001 60	0.649
0.010 35	0.001 60	0.610
0.012 94	0.001 60	0.563
0.015 52	0.001 60	0.520

**Table 3.** Curve-Resolving Data for Diluted Eph Solutions of Methyl Acetate in CHEX

vol fract Eph	vol fract MAC	fract of free carbonyl
0.002 87	0.001 60	0.765
0.004 01	0.001 60	0.698
0.005 73	0.001 60	0.639
0.008 60	0.001 60	0.560
0.011 46	0.001 60	0.500
0.014 33	0.001 60	0.452

**Table 4.** Screening Calculation Results for Concentrated Eph Solutions of Hyperbranched Acetylated Ester Where  $K_A^{12STD} = 113$  and  $K_A^{13STD} = 169$

polymer	$\gamma^{12}$	$\gamma_S^{12}$	$\gamma^{13}$	$\gamma_S^{13}$
generation 2	0.81	0.76	0.41	0.24
generation 4	0.83	0.78	0.58	0.46
generation 5	0.84	0.79	0.65	0.55

and the measured fraction free carbonyls are listed in Tables 2 and 3.

To calculate the interassociation equilibrium constants, we can directly use these data in the computer program "Fit K" developed by Dr J. F. Graf.<sup>9</sup> The necessary input includes the self-association equilibrium constants for Eph ( $K_2 = 16.2$ ,  $K_B = 51.4$  dimensionless units), the molar volumes of Eph, MTA, MAC, and CHEX (130, 79.5, 133, 108 cm<sup>3</sup> mol<sup>-1</sup>, respectively), and the volume fractions of Eph, MTA, and MAC in the mixtures. To make it convenient to compare equilibrium constants among single phase polymer blends or solutions, we scaled these dimensionless equilibrium constants to a common reference molar volume of 100 cm<sup>3</sup>/mol at 25 °C,  $K_A^{STD}$ . Least-squares fits for the equation describing the fraction free of carbonyl groups as a function of Eph volume fraction, illustrated in Figures 6 and 7, yielded a value of  $K_A^{STD} = 113$  dimensionless units for Eph/MTA and  $K_A^{STD} = 169$  dimensionless units for Eph/MAc, representing the intrinsic equilibrium constants for the internal and external repeat units of the hyperbranched polyester, respectively. The latter value is essentially identical to what we obtained previously for Eph/ethyl isobutyrate mixtures, as we anticipated it would given the essentially equal accessibility of the ester group in these molecules.

**Screening in Hyperbranched Molecules.** With the known values for intrinsic equilibrium constants  $K_A^{12}$  and  $K_A^{13}$ , we can calculate the "screening" or "accessibility" factors  $\gamma^{12}$  and  $\gamma^{13}$ , and compare these results to what we obtained for linear polymers. An example of the results of fitting  $\Phi_{B1}$ ,  $\gamma^{12}$ , and  $\gamma^{13}$  to the experimental data points is shown in Figure 8. The factor  $\gamma$  has two components, the first of which is a "connectivity" factor,  $\gamma_1$ , that manifests itself in the use of surface site fractions. If we assume a lattice co-ordination number of 9, an average value determined by Bernal,<sup>17</sup> then  $\gamma_1$

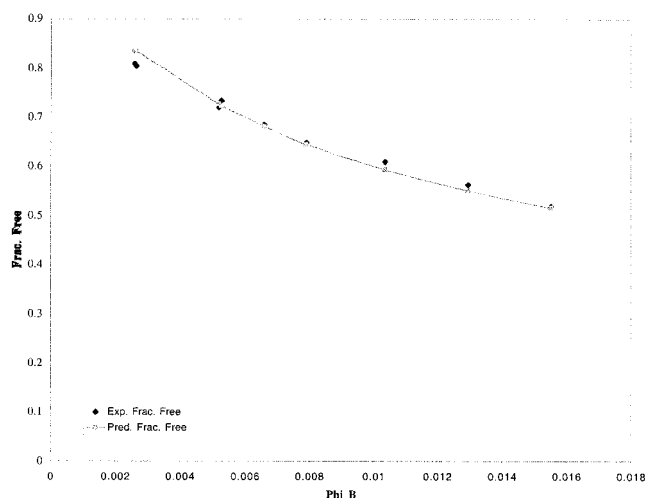


**Figure 6.** Least square fit from the program "Fit K" for dilute Eph/MTA in CHEX, resulting in the interassociation equilibrium constant  $K_A^{\text{STD}} = 113$ .

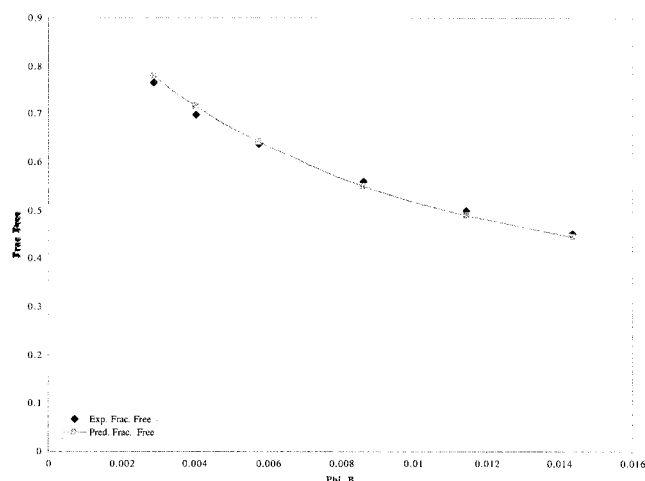


**Figure 7.** Least square fit from the program "Fit K" for dilute Eph/Mac in CHEX, resulting in the interassociation equilibrium constant  $K_A^{\text{STD}} = 169$ .

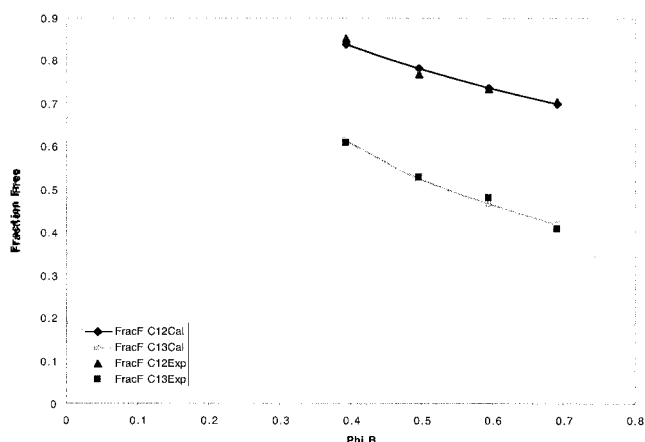


**Figure 8.** Best-fitted result for evaluating  $\Phi_B$ ,  $\gamma^{12}$ , and  $\gamma^{13}$  in concentrated Eph solutions of hyperbranched acetylated g 5 ester where  $K_A^{12\text{STD}} = 113$  and  $K_A^{13\text{STD}} = 169$ .

has a constant value of 0.22. The other component of  $\gamma$ ,  $\gamma_S$ , accounts for the fraction of same chain contacts, and this is the quantity that would be expected to vary significantly with chain architecture and generation number. For linear polymers we have found experimentally that  $\gamma_S \sim 0.3$ , close to values obtained by simula-

tions by Kumar.<sup>2</sup> As shown in Table 4, the value of  $\gamma_S$  for the internal carbonyl groups is far larger than this, of the order of 0.8 (but keep in mind that the exact value is sensitive to the value of  $K_A$  and presumably accumulates any errors in our experiments and assumptions). It is interesting that the values of  $\gamma_S^{12}$  are within error the same, indicating that the accessibility of the internal groups in these dendrimer-like molecules are equally (in)accessible or screened. The terminal groups are much more accessible, as would be expected, but the degree of screening increases drastically with generation number, even in this limited range.

## Conclusions

We believe we are able to successfully measure the relative accessibility of the internal and terminal carbonyl groups in hyperbranched polyester in terms of a "screening factor" evaluated from the degree of hydrocarbon bonding measured by FT-IR spectrometer. The screening factor for the groups in the interior of the molecules is much larger than for equivalent groups in linear polymers, but does not vary significantly with generation number. In contrast, in low generation number molecules the terminal groups are about as accessible as those in linear polymers, but these groups become less accessible as the generation number increases, presumably because the molecule folds back on itself to some degree resulting in a more compact, globular shape and hence more highly screened terminal groups.

**Acknowledgment.** The authors gratefully acknowledge the financial support of the national Science Foundation, Polymers Program.

## References and Notes

- (1) Coleman, M. M.; Painter, P. C. *Prog. Polym. Sci.* **1995**, *20*, 1.
- (2) Painter, P. C.; Veytsman, B.; Kumar, S.; Shenoy, S.; Graf, J. F.; Xu, Y.; Coleman, M. M. *Macromolecules* **1997**, *30*, 932.
- (3) Coleman, M. M.; Narvett, L. A.; Park, Y. H.; Painter, P. C. *J. Macromol. Sci.-Phys.* **1998**, *B37*, 283.
- (4) Coleman, M. M.; Pehlert, G. J.; Painter, P. C. *Macromolecules* **1996**, *29*, 6820.
- (5) Pehlert, G. J.; Painter, P. C.; Veytsman, B.; Coleman, M. M. *Macromolecules* **1997**, *30*, 3671.
- (6) Coleman, M. M.; Graf, J. F.; Painter, P. C. *Specific Interactions and the Miscibility of Polymer Blends*; Technomic Publishing: Lancaster, PA, 1991.
- (7) Hu, Y.; Painter, P. C.; Coleman, M. M.; Butera, R. J. *Macromolecules* **1998**, *31*, 3394.
- (8) De Gennes, P. G.; Hervet, H. *J. Phys. (Paris)* **1983**, *44*, L351.
- (9) Lescanec, L.; Muthukumar, M. *Macromolecules* **1990**, *23*, 2280.
- (10) Mansfield, L.; Klushin, L. I. *Macromolecules* **1993**, *26*, 4262.
- (11) Mansfield, L.; Klushin, L. I. *J. Phys. Chem.* **1992**, *96*, 3994.
- (12) Murat, M.; Grest, G. S. *Macromolecules* **1996**, *23*, 1278.
- (13) Boris, D.; Rubinstein, M. *Macromolecules* **1996**, *29*, 7251.
- (14) Wooley, K. L.; Klug, C. A.; Tasaki, K.; Schaefer, J. *J. Am. Chem. Soc.* **1997**, *119*, 53.
- (15) Painter, P. C.; Pruthitkul, R.; Coleman, M. M. *Macromol. Symp.* **1999**, *141*, 57-67.
- (16) Coleman, M. M.; Painter, P. C. In *Polymer Characterization Techniques and their Application to blends*, Simon, G. P., Ed.; American Chemical Society: Washington, DC, Chapter 6, in press.
- (17) Bernal, J. D. *Liquids: Structure, Properties, Solid Interactions*; T. J. Hughel, Ed.; Elsevier: Amsterdam, 1965.